

Elimination of the Effect of Vignetting for BER Performance Improvement in MIMO Optical Wireless Systems

Blessy Juliet.J, PG Student, DMI College of Engineering, Palanchur, Chennai-600 123

Guided by,

C.J. Profun, Assistant Professor, DMI College of Engineering, Palanchur, Chennai-600 123

Abstract -- Recently, the demand for high speed wireless multimedia services has grown to a great level. Multiple-Input Multiple-Output (MIMO) Optical Wireless Communication (OWC) can be an excellent supplemental technology to Radio Frequency (RF) links to achieve high transmission rates. One form of MIMO OWC is a pixelated imaging system which transmits information via a series of pixelated image frames. In order to be resilient to spatial distortions, pixelated systems can encode data using spatial orthogonal frequency division multiplexing. The Vignetting effect reduces the performance of a MIMO wireless communication system. A gradual fall-off in illumination at the edges of a received image will occur due to the Vignetting effect. The Vignetting effect causes attenuation as well as Inter-Carrier-Interference (ICI) in the spatial frequency domain. For a given constellation size, Spatial Asymmetrically Clipped Optical OFDM (SACO-OFDM) is more robust to Vignetting than Spatial DC-biased Optical OFDM (SDCO-OFDM). Moreover, for the case of SDCO-OFDM, the very large zeroth subcarrier causes severe ICI in its neighbourhood causing flattening of the Bit Error Rate (BER) curves. The BER performance can also be improved by applying a Vignetting Estimation and Equalization scheme. It is shown that equalized SACO-OFDM with 256-QAM has the same overall data rate as equalized SDCO-OFDM using 16-QAM, but requires less optical power.

Keywords: Optical Wireless Communication, MIMO, OFDM, Spatial OFDM, Vignetting, BER, ICI, Attenuation.

I. INTRODUCTION

OPTICAL wireless communication (OWC) systems can be used as an alternative to radio frequency systems for short range indoor communications. OWC has several appealing

attributes including low cost, high security, unlicensed bandwidth and simplicity. Multiple-input multiple-output (MIMO) OWC systems have the potential to provide higher data rates than their single-input single-output counterparts. However, research has shown that non-imaging MIMO systems provide little diversity gain. The use of imaging rather than non-imaging systems may provide a solution to this problem. One form of MIMO imaging scheme is a pixelated system, where the transmitter transmits a series of pixelated images, and a lens along with an array of photodetecting elements reproduces the images at the receiver. Such systems have the potential to provide high data rate transmission by exploiting spatial diversity at a large scale. Most pixelated systems use Spatial Orthogonal Frequency Division Multiplexing in the 2-D spatial domain. Spatial Asymmetrically Clipped Optical OFDM (SACO-OFDM) and Spatial DC-biased Optical OFDM (SDCO-OFDM) are two forms of Spatial OFDM that have been developed for MIMO imaging communication. A pixelated system can be impaired by Vignetting which is the gradual illumination fall-off from the centre to the corners of the received images. The Vignetting effect introduces Attenuation and ICI in the spatial frequency domain, resulting in bit errors in the Pixelated MIMO Optical wireless systems.

II. PIXELATED OPTICAL SYSTEMS

A Pixelated MIMO Optical Wireless System (OWC) makes use of the Imaging technique to provide high data rates.

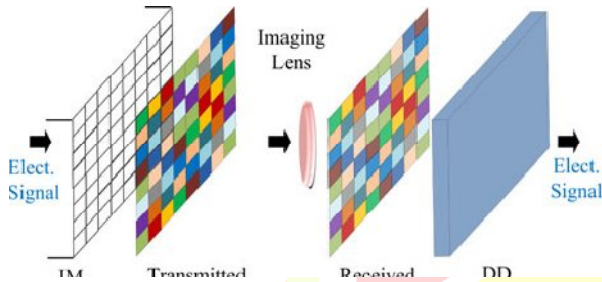


Fig. 1. Pixelated MIMO wireless communication system.

It is often said that “a picture is worth a thousand words”. The Pixelated MIMO Optical Wireless System makes use of this concept to create a high-rate wireless optical communication channel. In a pixelated system as shown in Fig. 1, the transmitter consists of a 2-D array of optical transmitters which send information encoded as a sequence of images. Liquid crystal displays (LCDs) and light emitting diodes (LEDs) are some examples of intensity modulators photo-detectors that detects the coded images. Charge-coupled device (CCD) cameras, arrays of photodiodes, Complimentary Metal–Oxide–Semiconductor imagers are some of the devices which can be used as Direct Detection (DD) receivers. LCDs and cameras are widely available in many handheld devices including laptops, tablet computers, personal digital assistants, and smart phones; and this creates a great opportunity for pixelated wireless communication. LCD camera links are attractive candidates for near field communication applications including mobile advertisement, data exchange and secure communication in military applications. A possible outdoor application of a pixelated system is in intelligent transportation systems, where LED traffic lights or LED automobile headlights can be used to transmit driver assistance information, which can be decoded by a vehicle mounted with a camera.

The pixelated wireless Optical channel is ideally suited to applications that require high-speed short range communication links, in which a line-of-sight is available. For interconnect and data exchange applications, the pixelated channel is attractive due to the availability of moderately priced components, unregulated bandwidth, compact size, and freedom from near-field effects in current radio links. A suitable area of application of the pixelated Optical channel is in situations that require strict signal containment. Examples of such applications include communications within a room or in some enclosure, or

perhaps between two communicating parties concerned about radiating to an unauthorized third party.

III. VIGNETTING EFFECT

In practice, several factors limit the performance of a pixelated system namely linear misalignment, channel noise, and defocus blur. A pixelated system can also be impaired by ‘vignetting’ which is the gradual illumination fall-off from the centre to the corners of the received images. It is a reduction of an image’s brightness or saturation at the periphery compared to the image center. In photography and optics, vignetting is often an unintended and undesired effect caused by camera settings or lens limitations. This is because, depending on the spatial positions of the IM transmitter elements, there is a variation in the intensity received by the receiver imaging lens. The level of vignetting depends on the geometry of the lens optics, aperture settings, and other optical properties of the receiver. The most prominent factors that contribute to vignetting in this type of imaging system are ‘cosine-fourth radiometric effect’, and the blocking of the transmitted light by the receiver elements. In a pixelated system, the information is encoded on the intensity of the transmitted images, and hence vignetting can result in incorrect data recovery at the receiver. Vignetting causes attenuation and InterCarrier interference (ICI) in the spatial frequency domain, resulting in bit errors, thereby reducing the Bit Error Rate (BER) Performance of the Pixelated MIMO Optical System.

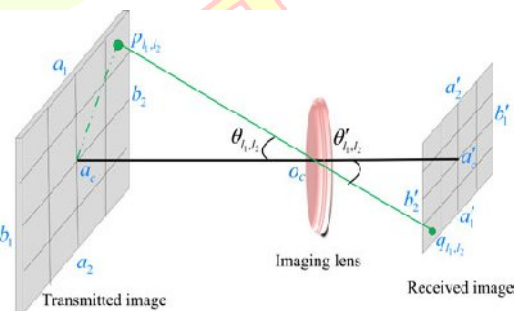


Fig. 2. Illustration of pixelated MIMO system using imaging lens.

From Fig. 2, $P_{h,j}$ is the transmitted frame and $P'_{h,j}$ is the corresponding image of the received frame. The centre of the receiver lens opening is represented by a_c . The transmitted light signal from any transmitted pixel, $P_{h,j}$, creates an angle, $\theta_{h,j}$, to the optical axis, a_c . The corresponding received pixel, $P'_{h,j}$, is also off-axis by $\theta'_{h,j}$. Next, an expression for the received pixels in terms of the

transmitted pixel is obtained. With these assumptions, the intensities of the received pixels, I_r , can be approximately represented as the intensities of the transmitted pixels, I_t , scaled by the vignetting function, V , as follows,

$$(1)$$

The term V for any pixel, (x, y) , can be expressed in the following format:

$$(2)$$

where, r is the distance between the centre of the transmitted image, (x_c, y_c) , and the pixel, (x, y) , and R is the

distance between the lens centre and the image plane. The vignetting function tends to unity for the case where, $r \ll R$, or $\theta \ll \theta_c$. Consequently, the amount of vignetting for any particular transmitter and receiver setup depends on the two ratios:

$$\frac{r}{R} \quad \text{and} \quad \frac{D}{2R} \quad (3)$$

where, D and R are the height and width of the transmitted image. Pixelated systems have potential usage in near field communication (3.8) where the ratios r/R and $D/2R$ are not negligible, and the amount of vignetting may be considerable.

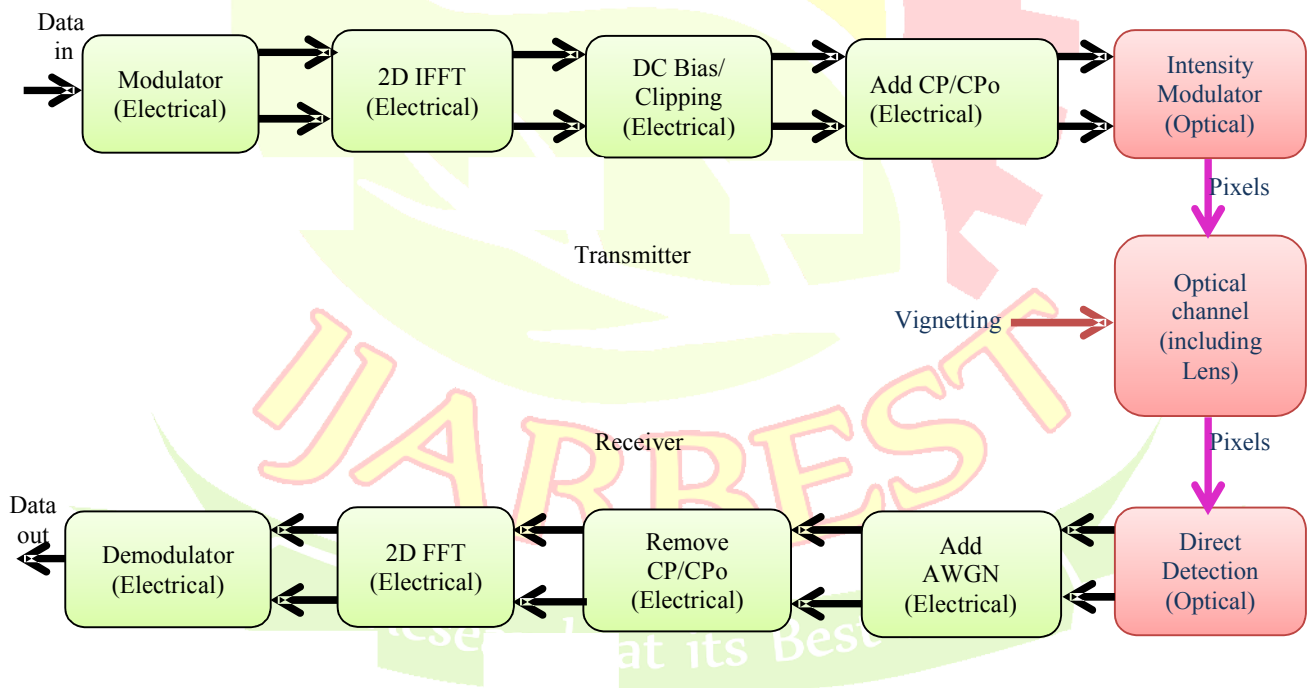


Fig. 3. Block diagram of a spatial OFDM system.

III. SPATIAL OFDM-BASED PIXELATED SYSTEM

Most pixelated systems use ‘spatial orthogonal frequency division multiplexing (OFDM)’ in the 2-D spatial domain. In conventional OFDM, information is carried in the 1D time domain, whereas in spatial OFDM orthogonal spatial frequency domain subcarriers are used to carry the data.

Compared to systems that encode data directly in the spatial domain, spatial OFDM based systems have the potential to be more resilient to spatial impairments. A cyclic prefix (CP) and a cyclic postfix (CPo) can be appended around the borders of the spatial OFDM transmitted frames, to make them tolerant to linear misalignment within the range of CP and CPo.

Fig. 3 shows the block diagram of a generalized spatial OFDM system. In SACO-OFDM, for each transmitted frame, the input data is mapped onto the N_1 by N_2 matrix of constellation points given by,

$$X = \begin{matrix} & \dots & & \dots & \\ & & & & \end{matrix} \quad (4)$$

The elements of matrix, X, are selected from the signal constellation being used. To ensure a real output signal from the 2-D inverse fast Fourier transform (2-D IFFT), the input matrix must have Hermitian symmetry. The data must also be mapped into the odd-index columns of X and the even-index columns set to zero, so that clipping noise does not affect the wanted signal. Assuming that both N_1 and N_2 are even integers, the Hermitian symmetry for X can be defined as follows:

$$(5)$$

where, k_1 and k_2 are the row and column indices respectively and 'x' is the complex conjugate operator. Next the 2-D IFFT is computed. For SACO-OFDM, The 2-D IFFT output is then clipped at the zero amplitude level to give,

$$(6)$$

where is the 2-D IFFT output and is the signal after clipping. In SDCO-OFDM, X is also constrained to have Hermitian symmetry. Unlike SACO-OFDM, in SDCO-OFDM data is mapped to both odd and even subcarriers of X. A dc bias, b_{DC} , is added to the IFFT output. Because of the Gaussian distribution of the spatial OFDM signal before clipping, even with a large dc bias, there will be some values for which the signal is negative. These are clipped at the zero amplitude level, but this causes clipping noise degrading the overall performance. The resultant SDCO-OFDM signal is given by,

$$(7)$$

where, μ is a constant, and is the standard deviation of . For both SACO-OFDM and SDCO-OFDM, a CP and a CPo are added to both the rows and the columns of the signal . The last block in the transmitter is the IM block where the real, positive spatial OFDM signal is used to modulate the optical intensity. The intensity of the transmitted pixels, , is given by,

$$(8)$$

where, ζ is the electrical-to-optical conversion efficiency. The receiver performs the inverse operations to the transmitter. The received pixels, , are converted back to an electrical signal by the DD detectors. The resultant electrical signal is given by,

$$(9)$$

where, is the responsivity of the photodetecting elements and is the channel noise, composed of shot noise and thermal noise, added in the electrical domain. In the pixelated systems considered, it is shown that the channel noise can be modeled as additive white Gaussian noise (AWGN). A 2-D FFT is then performed to give Y, the noisy received spatial frequency domain signal from which the data is recovered.

IV. PROPOSED LMMSE EQUALIZER

Vignetting Estimation and Equalization is used in the Spatial OFDM-based Optical Wireless System to reduce the effects of Vignetting such as increased attenuation, increased InterCarrier Interference (ICI) and reduced BER Performance. Channel estimation is a key technology for wireless optical communication (WOC) systems. Channel equalization is the process of reducing amplitude, frequency and phase distortion in a channel (3.3) the intent of improving transmission performance. Channel Estimation and Equalization for vignetting reduction are performed using the Linear Minimum Mean Square Error (LMMSE) algorithm. The LMMSE is optimum in minimizing Mean Square Error (MSE). The criterion used in this algorithm is to minimize the Mean Square Error (MSE) between the desired equalizer output and the actual equalizer output.

In Optical Wireless Systems Using Spatial OFDM, the pilot is sent in all sub-carriers with a specific period. Assuming the channel is constant during the block, it is insensitive to frequency selectivity. Since the pilots are sent at all carriers, there is no interpolation error.

$$\text{where } X = \text{diag} \{x_0, x_1, \dots, x_{N-1}\} \quad (10)$$

where x_i is the pilot value sent at the i^{th} sub-carrier and y_i is the value received at the i^{th} sub-carrier. If the time domain channel vector g is Gaussian and uncorrelated with the channel noise, the frequency-domain LMMSE estimate of g is given by,

$$h_{LMMSE} = FR_{gy}R_{yy}^{-1} \quad \text{where} \quad F = \begin{bmatrix} W_N^{00} & \dots & W_N^{0(N-1)} \\ \vdots & \ddots & \vdots \\ W_N^{(N-1)0} & \dots & W_N^{(N-1)(N-1)} \end{bmatrix} \quad \text{and} \quad (11)$$

$$W_N^{nk} = \frac{1}{N} e^{-j2\pi \frac{n}{N}k}$$

where R_{gy} and R_{yy} is cross covariance matrix between g and y and the auto-covariance matrix of y respectively. When the channel is slow fading, the channel estimation inside the block can be updated using the decision feedback equalizer at each sub-carrier. Decision feedback equalizer for the k^{th} sub-carrier can be described as follows:

- The channel response at the k^{th} sub-carrier estimated from the previous symbol $\{H_e(k)\}$ is used to find the estimated transmitted signal $\{X_e(k)\}$.

$$X_e(k) = \frac{Y(k)}{H_e(k)} \quad k = 0, 1, \dots, N-1 \quad (12)$$

- $\{X_e(k)\}$ is mapped to the binary data through “signal demapper” and then obtained back through “signal mapper” as $\{X_{\text{pure}}(k)\}$.
- The estimated channel $\{H_e(k)\}$ is updated by:

$$H_e(k) = \frac{Y(k)}{X_{\text{pure}}(k)} \quad k = 0, 1, \dots, N-1 \quad (13)$$

Since the decision feedback equalizer has to assume that the decisions are correct, the fast fading channel will cause the complete loss of estimated channel parameters. Therefore, as the channel fading becomes faster, there happens to be a compromise between the estimation error due to the interpolation and the error due to loss of channel tracking. For fast fading channels, the comb-type based channel estimation performs much better. LMMSE Equalizer is used

for Data Estimation (Equalization), Channel Estimation and Channel Shortening.

V. RESULTS

The Effect of Vignetting in Spatial OFDM-based Pixelated Optical Wireless systems using the proposed LMMSE Equalization is simulated using MATLAB in windows 8 Operating Platform and the following results are obtained.

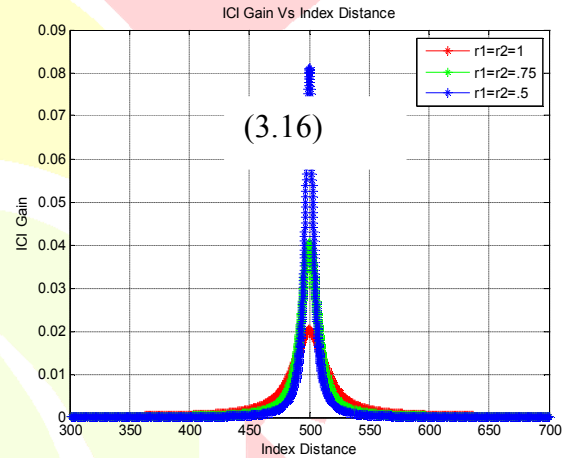


Fig. 4. ICI gain, versus \tilde{k}^2

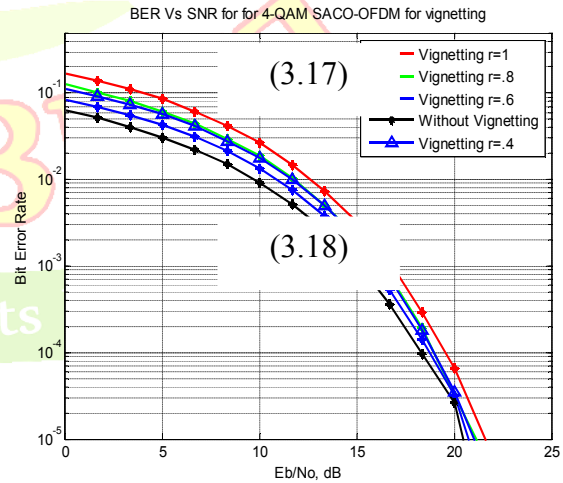


Fig. 5. BER versus E_b/N_0 for 4-QAM SACO-OFDM for vignetting

Fig. 4 shows the absolute values of ICI Gain versus \tilde{k}^2 for $M = N = 256$, $\tilde{k}_1 = 0$, and for three levels of vignetting. It is

clear that the values of \tilde{k}_2 are significant only for small values of \tilde{k}_1 , and that the peak is at $\tilde{k}_2 = \pm 1$. For other values of \tilde{k}_1 , the graphs have a similar form but the absolute values are smaller. In both SACO-OFDM and SDCO-OFDM, the zeroth subcarrier has the largest amplitude and therefore makes a greater ICI contribution than any other subcarrier. Consequently, the subcarriers close to the zeroth one experience severe ICI. This is more pronounced in SDCO-OFDM, where the zeroth subcarrier has very large amplitude resulting from the dc bias. Fig. 5 shows the BER for 4-QAM SACO-OFDM as a function of E_b/N_0 , the received electrical energy per bit to single-sided noise spectral density, where $N_0 = E\{ \dots \}$. The plots are for 256×256 subcarriers and show that when the ratio, r , has values of 0.4, 0.6, 0.8 and 1, the performance at a BER of 10^{-4} is degraded by 0.4 dB, 0.8 dB, 1.6 dB and 2.3 dB, respectively compared to a vignetting-free system. Fig. 6 shows the BER versus E_b/N_0 for both systems for 4-QAM and

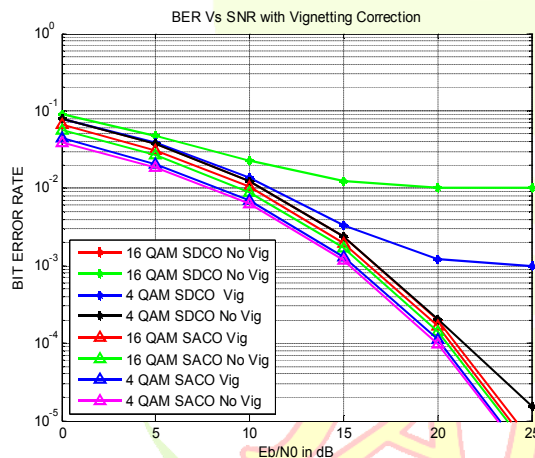


Fig. 6. BER versus E_b/N_0 for SACO-OFDM and SDCO-OFDM

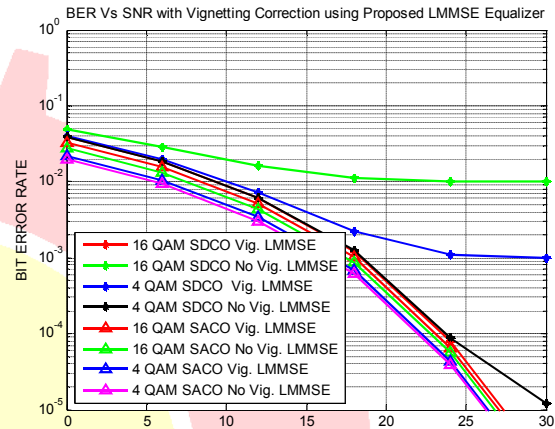


Fig. 7. BER versus E_b/N_0 using proposed LMMSE equalizer

16-QAM with and without vignetting. All the plots are for 256×256 subcarriers and for $r = 1$. It also shows that for 4-QAM, the BER degradation is more in SDCO-OFDM than SACO-OFDM. The BER curve for SDCO-OFDM flattens out. This is because for SDCO-OFDM, each subcarrier experiences significant interference from its adjacent subcarriers, whereas for SACO-OFDM, the data-carrying odd subcarriers suffer less interference from their adjacent even subcarriers. Fig. 7. shows the effect of equalization for SACO-OFDM and SDCO-OFDM systems for $r = 1$. The use of an equalizer improves the BER performance by compensating for the vignetting-induced attenuation. As the BER degradation is greater in 16-QAM than 4-QAM, the effect of the equalizer is also greater for 16-QAM. It can be seen that the error floor is lower for a larger number of subcarriers. This is because the error floor is due to the subcarriers close to the zeroth subcarrier. Fig. 8 shows the BER versus E_b/N_0 of both SACO-OFDM AND SDCO-OFDM with vignetting correction using the proposed Equalizer with Higher Order QAM Modulation. Fig. 8 shows

BER Vs SNR with Vignetting Correction using Proposed LMMSE Equalizer with High Order QAM

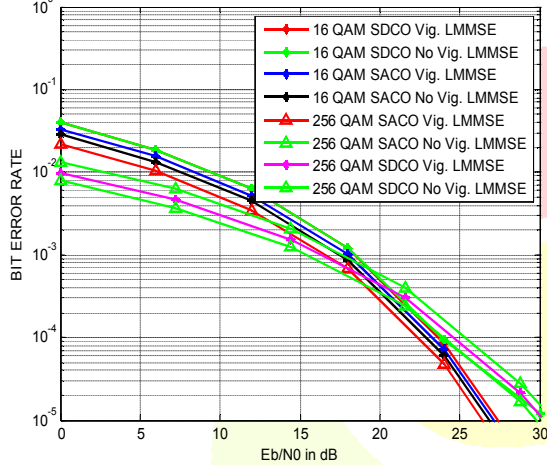


Fig. 8. BER Performance of Proposed LMMSE Equalizer with Higher Order QAM

the BER performance levels for the 16-QAM and 256-QAM Modulations. It is shown that 256-QAM shows the best BER performance.

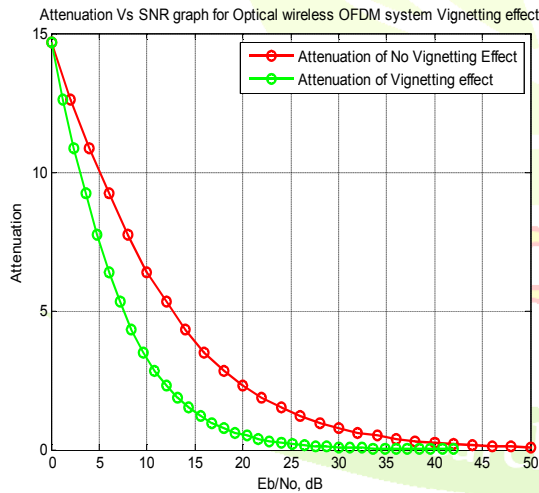


Fig. 9. Attenuation profile with and without vignetting

Fig. 9 shows the distortion introduced to the transmitted signals can be mitigated on the condition that the signal attenuation factor is known at the receiver. Here, to alleviate the distortion and disclose the signal feature of peak-cancellation combined spatial OFDM signals, the signal attenuation factor is analyzed and hence evaluated.

VI. CONCLUSION

The Proposed work analyzes the impact of vignetting on a Spatial OFDM based pixelated system and its reduction using the LMMSE Vignetting Estimation and Equalization algorithm. It is shown that vignetting introduces Attenuation and ICI in the spatial frequency domain, resulting in bit errors, thereby degrading the BER performance. The LMMSE algorithm is applied to reduce the effect of vignetting. This method estimates and equalizes vignetting in the spatial domain and provides improvement in the system BER performance. The BER performances of SACO-OFDM and SDCO-OFDM are compared and it shows that SACO-OFDM shows improved vignetting robustness than SDCO-OFDM. Also, 256-QAM modulation is implemented, which shows further BER improvement.

REFERENCES

- [1] D. O'Brien, R. Turnbull, H. L. Minh, G. Faulkner, O. Bouchet, P. Porcon, M. E. Tabach, E. Gueutier, M. Wolf, L. Grobe, and J. Li, "High-speed optical wireless demonstrators: Conclusions and future directions," *J. Lightw. Technol.*, vol. 30, no. 13, pp. 2181–2187, Jul. 2012.
- [2] J. Kahn and J. Barry, "Wireless infrared communications," *Proc. IEEE*, vol. 85, pp. 265–298, 1997.
- [3] D. O'Brien, M. Katz, P. Wang, K. Kalliojarvi, S. Arnon, M. Matsumoto, R. Green, and S. Jivkova, "Short-range optical wireless communications," in *Technologies for the Wireless Future: Wireless World Research Forum*, 2nd ed, New York, NY, USA: Wiley, 2006, vol. 2, pp. 277–296.
- [4] K. Langer and J. Grubor, "Recent developments in optical wireless communications using infrared and visible light," presented at the Int. Conf. Transparent Optical Networks, Rome, Italy, Jul. 2007.
- [5] R. J. Green, H. Joshi, M. D. Higgins, and M. S. Leeson, "Recent developments in indoor optical wireless systems," *IET Commun.*, vol. 2, pp. 3–10, 2008.
- [6] M. Kavehrad, "Sustainable energy-efficient wireless applications using light," *IEEE Commun. Mag.*, vol. 48, no. 12, pp. 66–73, Dec. 2010.
- [7] S. Hranilovic, *Wireless Optical Communication Systems*. New York, NY, USA: Springer, 2004.
- [8] H. Elgala, R. Mesleh, and H. Haas, "Indoor optical wireless communication: Potential and state-of-the-art," *IEEE Commun. Mag.*, vol. 49, no. 9, pp. 56–62, Sep. 2011.
- [9] L. Zeng, D. O'Brien, H. Minh, G. Faulkner, K. Lee, D. Jung, Y. Oh, and E. T. Won, "High data rate multiple input multiple output (MIMO) optical wireless communications using white LED lighting," *IEEE J. Sel. Areas Commun.*, vol. 27, no. 9, pp. 1654–1662, Dec. 2009.
- [10] H. B. C. Wook, T. Komine, S. Haruyama, and M. Nakagawa, "Visible light communication with LED-based traffic lights using 2-dimensional image sensor," in *Proc. IEEE Consumer Commun. Netw. Conf.*, Jan. 8–10, 2006, pp. 243–247.



- [11] A. Ashok, M. Gruteser, N. B. Mandayam, J. Silva, M. Varga, and K. J. Dana, "Challenge: Mobile optical networks through visual MIMO," in Proc. Int. Conf. Mobile Comput. Netw., Chicago, IL, USA, Sep. 20–24, 2010, pp. 105–112.
- [12] S. Hranilovic and F. R. Kschischang, "Short-range wireless optical communication using pixelated transmitters and imaging receivers," in Proc. IEEE Int. Conf. Commun., 2004, pp. 891–895.
- [13] S. Hranilovic and F. R. Kschischang, "A pixelated MIMO wireless optical communication system," IEEE J. Sel. Topics Quantum Electron., vol. 12, no. 4, pp. 859–874, Jul./Aug. 2006.
- [14] M. D. A. Mohamed and S. Hranilovic, "Two-dimensional binary half-toned optical intensity channels," IET Commun., vol. 2, pp. 11–17, 2008.
- [15] M. D. A. Mohamed, A. Dabbo, and S. Hranilovic, "MIMO Optical wireless channels using half-toning," presented at the IEEE Int. Conf. on Communications, Beijing, China, May 2008.
- [16] S. D. Perli, N. Ahmed, and D. Katabi, "PixNet : LCD-Camera pairs as communication links," presented at the Special Interest Group on Data Communication, New Delhi, India, Aug. 2010.
- [17] S. D. Perli, N. Ahmed, and D. Katabi, "PixNet: Interference-free wireless links using LCD-camera pairs," presented at the Int. Conf. Mobile Computing and Networking, Chicago, IL, USA, Sep. 20–24, 2010.
- [18] C. C. Pei, Z. C. Zhang, W. X. Fang, and S. J. Zhang, "2D-DPSK for quasi diffuse pixelated wireless optical," in Proc. IEEE Int. Conf. Commun. Technol., Jinan, China, Sep. 25–28, 2011, pp. 556–559.
- [19] T. Hao, R. Zhou, and G. Xing, "COBRA: Color barcode streaming for smartphone systems," presented at the Int. Conf. Mobile Systems, Applications and Services, Lake District, U.K., Jun. 25–29, 2012.
- [20] M. R. H. Mondal, K. R. Panta, and J. Armstrong, "Performance of two dimensional asymmetrically clipped optical OFDM," in Proc. IEEE Globecom Workshops, Piscataway, NJ, USA, Dec. 2010, pp. 995–999.
- [21] M. R. H. Mondal and J. Armstrong, "Impact of linear misalignment on a spatial OFDM based pixelated system," presented at the Asia Pacific Conf. on Communications, Jeju Island, South Korea, Oct. 15–17, 2012.
- [22] M. R. H. Mondal and J. Armstrong, "The effect of defocus blur on a spatial OFDM optical wireless communication system," presented at the 14th Int. Conf. on Transparent Optical Networks, Coventry, U.K., Jul. 2–5, 2012.
- [23] A. Dabbo and S. Hranilovic, "Receiver design for wireless optical MIMO channels with magnification," presented at the 10th Int. Conf. on Telecommunications, Zagreb, Croatia, Jun. 8–10, 2009.
- [24] A. Dabbo and S. Hranilovic, "Multilevel error diffusion for wireless optical MIMO channels," presented at the 24th Biennial Symp. on Communications, Kingston, ON, Canada, Jun. 24–26, 2008.
- [25] W. Yuan, K. Dana, M. Varga, A. Ashok, M. Gruteser, and N. Mandayam, "Computer vision methods for visual MIMO optical system," in Proc. IEEE Comput. Soc. Conf. Comput. Vision Pattern Recog. Workshops, Colorado Springs, CO, USA, Jun. 2011, pp. 37–43.
- [26] W. Yuan, K. Dana, A. Ashok, M. Gruteser, and N. Mandayam, "Dynamic and invisible messaging for visual MIMO," in Proc. IEEE Workshop Appl. Comput. Vision, Colorado Springs, CO, USA, Jan. 2012, pp. 345–352.
- [27] A. Ashok, M. Gruteser, N. Mandayam, K. Taekyoung, Y. Wenjia, M. Varga, and K. Dana, "Rate adaptation in visual MIMO," in Proc. 8th Annu. IEEE Commun. Soc. Conf. Sensor, Mesh, Ad. Hoc. Commun. Netw., Salt Lake City, UT, USA, Jun. 2011, pp. 583–591.
- [28] M. Aggarwal, H. Hua, and N. Ahuja, "On cosine-fourth and vignetting effects in real lenses," presented at the Int. Conf. on Computer Vision, Vancouver, BC, Canada, Jul. 7–14, 2001.
- [29] V. N. Mahajan, Optical Imaging and Aberrations: Part I. Ray Geometrical Optics. Bellingham, WA, USA: SPIE, Jul. 1998.